



### **Full Length Article**

## **Estimation of Leaf Nitrogen Concentration in Wheat by the Combinations of Two Vegetation Indexes using HJ-CCD Images**

**Changwei Tan\*, Dunliang Wang, Jian Zhou, Ying Du, Ming Luo and Wenshan Guo\***

*Jiangsu Key Laboratory of Crop Genetics and Physiology/Co-Innovation Center for Modern Production Technology of Grain Crops, Yangzhou University, Yangzhou, China*

\*For correspondence: tanwei010@126.com; guows@yzu.edu.cn

### **Abstract**

To enhance the reliability of remote sensing evaluation model of leaf nitrogen concentration (LNC) in wheat, this paper analyzed the relationships of LNC at critical stages with the combinations of two vegetation indexes obtained from HJ-CCD images. The combined models were compared with the one-fold vegetation index model. The results demonstrated that N (SIPI, EVI), the normalization for SIPI and EVI, was practical to evaluate LNC at elongation stage with  $R^2$  and RMSE of 0.69 and 0.34, respectively, and superior to the one-fold vegetation index model with accuracy increased by 9.9%. D (PSRI, DVI), difference combination for PSRI and DVI, was practical to evaluate LNC at booting stage with  $R^2$  and RMSE of 0.71 and 0.18, respectively and superior to the one fold vegetation index model with increased accuracy by 15.2%. Normalization combination for SIPI and PSRI, namely N (SIPI, PSRI), was practical to evaluate LNC at anthesis with  $R^2$  and RMSE of 0.89 and 0.31, respectively and superior to the one fold vegetation index model with accuracy increased by 14.7%. In summary, N (SIPI, EVI), D (PSRI, DVI) and N (SIPI, PSRI) are potential indicators of LNC at different stages and can be a new method for more accurate evaluation of wheat growth. © 2018 Friends Science Publishers

**Keywords:** HJ-CCD images; Leaf nitrogen concentration; Vegetation indexes; Evaluation model; Wheat

### **Introduction**

Leaf nitrogen concentration (LNC) is used as a reference to measure growth conditions, output and quality of crop (Serrano *et al.*, 2002; Daniela *et al.*, 2009; Inoue *et al.*, 2012). How to acquire nitrogen concentration of crops accurately had become the hotspot of remote sensing crop monitoring research (Pinter Jr *et al.*, 2003; Ree, 2006; Martin *et al.*, 2008). Many experts and scholars had explored crops LNC based on different remote sensing data sources and put forward a variety of estimation methods of crops. The most common method of the nitrogen concentration was to derive spectral indexes by combining two or more characteristic wavebands into a simple ratio or into a more complicated formula based on algorithms and N-related plant physiological significance such as leaf nitrogen concentration (Hatfield *et al.*, 2008; Ollinger, 2011; Miphokasap *et al.*, 2012). Muharam *et al.* (2015b) developed an estimation model of canopy nitrogen concentration using field imaging spectroscopy. A remote sensing estimation model of crop LNC had been established by combining ground cover information and using canopy reflectance spectrum (Chen *et al.*, 2010; Muharam *et al.*, 2015a). Based on the near-infrared monitoring model of wheat LNC, it was discovered that the monitoring model based on wavelet neural network (WNN) was better than

those based on partial least squares (PLS) and back-propagation neural networks (BPNN) (Jacobi *et al.*, 2006). Most previous research focused on regression analysis of single vegetation index and agronomic parameter or a series of algorithms based on single vegetation index (Tarpley *et al.*, 2000; Morón *et al.*, 2007; Tan *et al.*, 2011; Tuia *et al.*, 2011; Bagheri *et al.*, 2013; Boegh *et al.*, 2013; Muharam *et al.*, 2015b). Researchers realized dynamic monitoring of crop LNC based on new characteristic parameters (e.g., slope and included angle) which were extracted from the hyperspectral reflectance curve of visible light-near infrared region using field investigation data (Daughtry *et al.*, 2000; Xu *et al.*, 2009). By analyzing the optimal weighted parameter composition, some parameters had the strongest response capability to spectral information of crop LNC, conducive to enhancing monitoring stability and estimation accuracy. In addition, some researches showed that the combination of red-edge wavelengths with very near infrared wavelengths provided good precision and accuracy for predicting LNC (Tarpley *et al.*, 2000). Daughtry *et al.* (2000) proposed a vegetation index named Modified Chlorophyll Absorption Ratio Index (MCARI) and applied it for canopy chlorophyll and nitrogen measurements. Ryu *et al.* (2011) established a multi-year PLS regression model for quantifying nitrogen content using hyperspectral data, and found that accuracy of the multi-year PLS regression

models was better than the multi-year models based on multiple linear regression.

This research aimed to put forward a new method of further improving the accuracy of remote sensing evaluation model of wheat LNC at critical stages, examine the effects of employing the combinations of two vegetation indexes to remotely evaluate LNC, and establish the quantitative evaluation models with high accuracy based on HJ-CCD images. Sensitive vegetation indexes or their combinations were adopted to analyze LNC and multispectral vegetation indexes at critical stages. The authors focused on the quantitative relationships of LNC with their differences, ratios and normalized combinations of two vegetation indexes obtained by HJ-CCD images. Based on the combinations of sensitive vegetation indexes, the evaluation of LNC was realized, which provides a new method for accurate crop cultivation and real-time acquisition of crop growth information.

## Materials and Methods

### Study Areas and Field Sampling

Test 1: The test was conducted in 2015 in Taixing, Jiangyan, Xinghua, and Dafeng in Jiangsu Province, China. In each study area, 15–20 sampling sites were set A total of 66 sampling points were designed.

Test 2: The test was conducted in 2016 in Taixin, Jiangyan, Xinghua, and Gaoyou in Jiangsu Province, China. In each study area, 30 sampling sites were set A total of 120 sampling points were designed.

Test 3: The test was conducted in 2017 in Yizheng, Jiangyan, Xinghua, Taixing, and Dafeng in Jiangsu Province, China. In each study area, 20–25 sampling sites were set A total of 114 sampling points were designed.

The study was carried out in the midland of Jiangsu Province (119°12' to 120°26' E, 32°2' to 33°16' N), which was an important wheat producing area in Jiangsu. The terrain is flat in this area. It is mainly affected by the subtropical monsoon climate, with an average annual rainfall of about 1000 mm and annual average sunshine of about 2,200 h. Rice was the dominant crop in study areas.

### Laboratory and Field Measurements

Sampling sites in Section 2.1 were uniformly distributed. For each sampling sites, location information was acquired by handheld GPS instrument made in Trimble Company. Test stages including elongation, booting, and flowering stages were determined by actual field investigation. Field survey showed that there was no significant difference in wheat growing conditions between 2015 and 2017 at the same periods. The sampling points were all set in large-area field areas with wheat uniform growth and the well managed fields. The sampling points were set at a distance of at least 60 m from the boundary of the field.

The sampling points set in the first period were applied to all subsequent periods. In the center of the experimental area, four rows (50 cm) of uniform wheat were selected. At the same time, carried out GPS positioning and recorded geographical information.

All collected samples were sent to laboratory timely to test LNC. 15–20 plants were collected at all sampling sites during different periods of wheat (elongation, booting and flowering stages). Leaf samples were dried, grinded, screened and dried again to test wheat LNC by Kjeldahl method.

### Remote Sensing Image Acquisition and Processing

The remote sensing images used in this study were HJ-CCD images obtained from Resource Satellite Application Center, China. 9 satellite image acquisition dates were elongation stage (20150311, 20160308 and 20170309), booting stage (20150413, 20160411 and 20170412) and flowering stage (20150425, 20160503 and 20170428).

ENVI5.0 software was used to process HJ-CCD images. Firstly, the rough correction of remote sensing images was performed based on the topographic maps of Jiangsu Province (scale: 1:100,000). Secondly, the images were geometrically fine-tuned based on the ground control points measured by the GPS. Finally, atmospheric corrections and reflectivity conversions were performed using an empirical linear transformation.

Representative water body of the study areas was used as a target for low reflectivity calibration and open cement pavement was used as a target for high reflectivity calibration. Satellite image (HJ-CCD) scaling was performed by manual calibration. The digital value (DN) images were converted to radiation images based on absolute calibration coefficient based on the following formula:

$$L = DN/a + L_0 \quad (1)$$

Here, L represented radiance, a was gains of absolute calibration coefficient and  $L_0$  was offset. L unit was  $W \cdot m^{-2} \cdot sr^{-1} \cdot \mu m^{-1}$ .

### Remote Sensing Vegetation Indexes

In this study, commonly used vegetation indexes related to LNC based from the literature were selected. We used ENVI 5.0 software to extract the spectral reflectance of the GPS-located sampling points. Next, combined with the existing satellite remote sensing index algorithm, the vegetation indexes were computed according to the formulas (Table 1).

### Combinations of Different Remote Sensing Vegetation Indexes

Eight common remote sensing vegetation indexes: NDVI, NRI, GNDVI, SIPI, PSRI, DVI, RVI and EVI

were used in present study. They were matched by differential calculations, ratio calculations, and normalization processing. Taking A and B as examples, the combinations were defined: D (A, B) = A-B, R (A, B) = A/B and N (A, B) = (A-B)/(A+B), respectively corresponding to difference, ratio and normalization combinations. Therefore, a total of 84 diverse and credible combinations were obtained.

### Data Analysis and Utilization

We used SPSS18.0 to analyze the correlation between different vegetation indexes and the combinations and LNC at different stages (elongation, booting and flowering stages). Based on the principle of strongest correlation, a variety of wheat LNC evaluation models were established during the main growth periods (exponential, linear, polynomial, logarithmic and power correlation models). Consequently, the relations diagram between predicted and measured LNC values was drawn to evaluate the established model. Accuracy of the remote sensing evaluation model was evaluated by degree of fitting ( $R^2$ ) and root mean square error (RMSE). Equation (2) was used to calculate RMSE. In addition, the spatial grade map of LNC distribution at critical stages was drawn.

$$RMSE = \sqrt{\frac{1}{n} \sum_{i=1}^n (y_i - \hat{y}_i)^2} \quad (2)$$

Here,  $y_i$  and  $\hat{y}_i$  represented observed values and simulated values, respectively;  $n$  was number of samples.

## Results

### Relationships of Vegetation Indexes and the Combinations with Wheat LNC

The normalization combination of SIPI and EVI, namely N (SIPI, EVI), had the highest correlation coefficient at the elongation stage in the combinations, and was better than one fold vegetation index (Table 2 and 3). N (SIPI, EVI) had stronger correlation ( $r=-0.78$ ) than R (SIPI, EVI) and D (SIPI, EVI). Therefore, LNC inversion by N (SIPI, EVI) was practical at elongation stage. At booting stage, D (PSRI, DVI) had stronger correlation ( $r=-0.72$ ) with LNC than R (GNDVI, DVI) and N (GNDVI, DVI), which were better than one fold vegetation indexes. D (PSRI, DVI) showed the strongest correlation ( $r=-0.72$ ), indicating that LNC inversion based on D (PSRI, DVI) at the booting stage was practical. At the flowering stage, N (SIPI, PSRI) showed the strongest correlation ( $r=0.81$ ). Therefore, the N (SIPI, PSRI) model was used to evaluate LNC of wheat at the flowering stage for the principle of simplicity.

### Establishment of Wheat LNC Model Based on Vegetation Index

Based on the strong correlation principle and above analysis results, N (SIPI, EVI), D (PSRI, DVI) and N (SIPI, PSRI) were chosen to evaluate LNC at elongation, booting and flowering stages, respectively. Then, the combined vegetation indexes were used as independent variables and LNC was used as the dependent variable to establish remote sensing evaluation models of wheat LNC by exponential, linear, polynomial, power and logarithmic modeling methods (Table 4).

The wheat LNC remote sensing evaluation model with the highest  $R^2$  value was measured at the elongation, booting and the flowering stages (Fig. 1). More precisely, the evaluation model of wheat LNC at elongation stage was established by polynomial method ( $R^2=0.65$ ). Although, the evaluation models of wheat LNC at booting stage established by polynomial ( $R^2=0.52$ ) and linear ( $R^2=0.52$ ) modeling methods were similar, the linear model was simpler and applied in this study. The evaluation model of wheat LNC at flowering stage was established by linear method ( $R^2=0.45$ ).

### Assessing the Combined Evaluation Models of Wheat LNC

To evaluate accuracy of the combined evaluation models, the relations between predicted and measured LNC values were quantitatively analyzed with 66 samples observed at elongation stage, booting stage and flowering stage in 2015. The three combined evaluation models were compared with corresponding one fold vegetation index models (Fig. 2).

It could be seen from comparison (elongation stage, booting stage and flowering stage) that the predicted LNC by the N (SIPI, EVI) evaluation model was highly correlated with measured LNC ( $R^2=0.69$ ,  $RMSE=0.34$ ). It was superior to the one fold vegetation index evaluation model and achieves 9.9% higher accuracy. Therefore, N (SIPI, EVI) was applicable to evaluate wheat LNC at elongation stage. Similarly, the D (PSRI, DVI) evaluation modeling showed  $R^2=0.71$ ,  $RMSE=0.18$  and growth accuracy =15.2%, indicating its applicability to evaluate wheat LNC at booting stage. At flowering, the N (SIPI, PSRI) model was more useful than one fold vegetation index models with  $R^2=0.89$ ,  $RMSE=0.31$  and growth accuracy = 14.7%. In summary, the combined model based on two vegetation indexes, used to evaluate LNC in wheat, could promote the evaluation accuracy, so that it was practical to provide a new application method for accurately evaluating crop growth in future.

### Mapping Spatial Distribution of Wheat LNC

According to Table 4, HJ-CCD images in 2017 and the formulas in Table 1, numerical values of sensitive variables were calculated correctly and effectively one by one.

**Table 1:** Common satellite remote sensing vegetation indexes

Vegetation index	Calculation formula
Normalized difference vegetation index (NDVI)	$NDVI = (B4 - B3) / (B4 + B3)$
Nitrogen reflectance index (NRI)	$NRI = (B2 - B3) / (B2 + B3)$
Green normalized difference vegetation index (GNDVI)	$GNDVI = (B4 - B2) / (B4 + B2)$
Structure intensive pigment index (SIPI)	$SIPI = (B4 - B1) / (B4 + B1)$
Plant senescence reflectance index (PSRI)	$PSRI = (B3 - B1) / B4$
Difference vegetation index (DVI)	$DVI = B4 - B3$
Ratio vegetation index (RVI)	$RVI = B4 / B3$
Enhanced vegetation index (EVI)	$EVI = 2.5 * (B4 - B3) / (B4 + 6 * B3 - 7.5 * B2 + 1)$

Note: B1, B2, B3 and B4 denoted spectrum reflectance at blue, green, red and near infrared bands, respectively. The same as below

**Table 2:** Correlation between vegetation indexes and LNC of wheat at critical stages

Vegetation indexes	NDVI	NRI	GNDVI	SIPI	PSRI	DVI	RVI	EVI
Elongation Stage	0.40**	0.43**	-0.27**	-0.18*	-0.34**	0.34**	0.43**	<b>0.70**</b>
Boot stage	<b>0.51**</b>	0.22**	-0.05	0.21*	-0.14	0.60**	0.41**	0.30**
Flowering stage	0.31**	0.09	-0.04	<b>0.67**</b>	-0.41**	0.18*	0.22**	-0.18**

Note: \*:  $P < 0.05$ ; \*\*:  $P < 0.01$ . The same as below

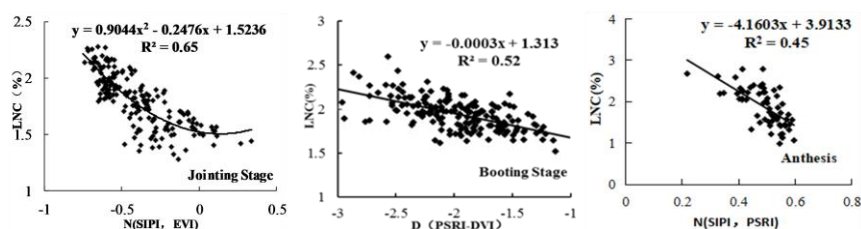


**Fig. 1:** Remote sensing evaluation model of wheat LNC at key stages

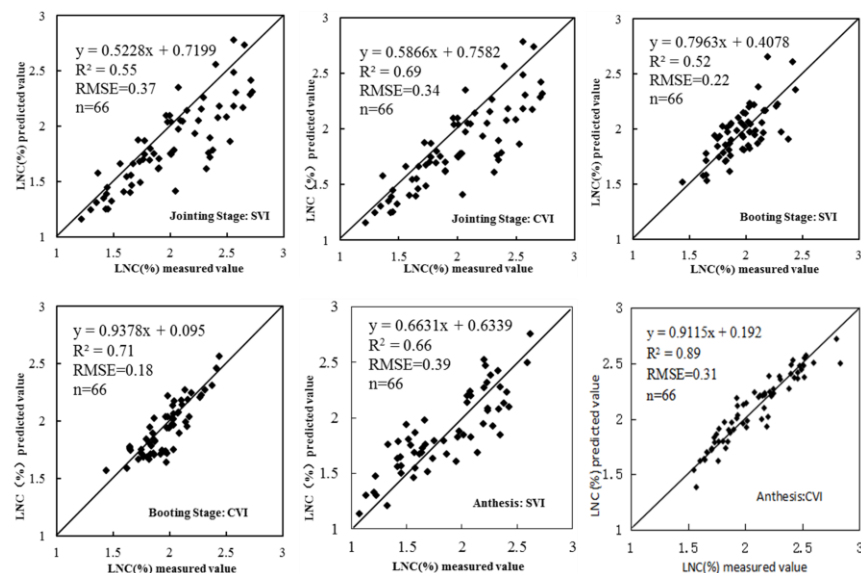


**Fig. 2:** Reliability of the evaluation models of wheat LNC at key stages

SVI: Single vegetation index; CVI: Combination of vegetation index

After creating mask images, sampling sites were positioned with GPS instrument and wheat-planting areas was classified by using supervised method. Field correction was performed to ensure classification accuracy of wheat-

planting areas. Overlaying the topographic vector maps of Jiangsu Province, the remote sensing evaluation maps of wheat LNC spatial distribution was drawn with ArcGIS10.2 software (Fig. 3).

**Table 3:** Correlation between combinations of vegetation indexes and wheat LNC at critical stages

Vegetation indexes combinations	Difference combination	Ratio combination	Normalization combination
(NDVI, NRI)	(0.19*, 0.45**, 0.31**)	(-0.42**, -0.15*, -0.02)	(-0.08, 0.0138, 0.08)
(NDVI, GNDVI)	(0.44**, 0.45**, 0.22**)	(0.44**, 0.56**, 0.21**)	(0.47**, 0.41**, 0.22**)
(NDVI, SIPI)	(0.47**, 0.36**, 0.16*)	(0.46**, 0.47**, 0.17*)	(0.52**, 0.34**, 0.17*)
(NDVI, PSRI)	(0.45**, 0.50**, 0.34**)	(0.25**, 0.50**, -0.01)	(0.47**, 0.38**, 0.40**)
(NDVI, DVI)	(-0.34**, -0.70**, -0.18*)	(0.14*, -0.07, 0.04)	(0.14*, -0.03, 0.04)
(NDVI, RVI)	(-0.42**, -0.38**, -0.15*)	(-0.23**, -0.01, 0.03)	(0.03, 0.01, 0.05)
(NDVI, EVI)	(-0.70**, -0.20*, 0.23**)	(-0.62**, -0.03, 0.20**)	(-0.64**, -0.05, 0.23**)
(NRI, GNDVI)	(0.42**, 0.19*, 0.06)	(0.40**, 0.14*, 0.12)	(0.38**, 0.23**, 0.12)
(NRI, SIPI)	(0.39**, 0.01, -0.15*)	(0.36**, 0.25**, 0.03)	(0.32**, 0.30**, 0.04)
(NRI, PSRI)	(0.47**, 0.23**, 0.29**)	(0.25**, 0.07, -0.01)	(-0.09, 0.02, 0.01)
(NRI, DVI)	(-0.34**, -0.72**, -0.18*)	(0.50**, 0.47**, -0.02)	(0.54**, 0.41**, -0.02)
(NRI, RVI)	(-0.41**, -0.40**, -0.21**)	(0.59**, 0.36**, -0.02)	(0.59**, 0.33**, -0.02)
(NRI, EVI)	(-0.70**, -0.26**, 0.18**)	(0.65**, 0.23**, 0.13*)	(-0.10, -0.02, 0.14*)
(GNDVI, SIPI)	(-0.03, -0.23**, -0.21**)	(-0.02, -0.32**, -0.20**)	(-0.03, -0.23**, -0.20**)
(GNDVI, PSRI)	(0.01, 0.01, 0.02)	(0.13, 0.05, -0.01)	(0.20**, 0.10, 0.40**)
(GNDVI, DVI)	(-0.34**, -0.70**, -0.18*)	(-0.38**, -0.69**, -0.20**)	(-0.43**, -0.50**, -0.20**)
(GNDVI, RVI)	(-0.41**, -0.41**, -0.24**)	(-0.48**, -0.48**, -0.23**)	(-0.37**, -0.37**, -0.24**)
(GNDVI, EVI)	(-0.71**, -0.27**, 0.18*)	(-0.71**, -0.26**, 0.09)	(-0.76**, -0.25**, 0.12)
(SIPI, PSRI)	(0.03, 0.24**, 0.29**)	(0.14*, 0.27**, -0.22)	(0.62**, 0.46**, <b>0.81**</b> )
(SIPI, DVI)	(-0.34**, -0.70**, -0.18*)	(-0.39**, -0.57**, -0.09)	(-0.45**, -0.40**, -0.09)
(SIPI, RVI)	(-0.45**, -0.40**, -0.20**)	(-0.58**, -0.38**, -0.12)	(-0.78**, -0.29**, -0.12)
(SIPI, EVI)	(-0.72**, -0.25**, 0.21**)	(-0.71**, -0.21**, 0.17*)	( <b>-0.78**</b> , -0.20**, 0.20**)
(PSRI, DVI)	(-0.34**, -0.72**, -0.18*)	(-0.40**, -0.60**, -0.39**)	(-0.46**, -0.46**, -0.39**)
(PSRI, RVI)	(-0.44**, -0.41**, -0.23**)	(-0.53**, -0.43**, -0.39**)	(-0.56**, -0.34**, -0.39**)
(PSRI, EVI)	(-0.71**, -0.27**, 0.17*)	(-0.64**, -0.26**, -0.36**)	(-0.70**, -0.24**, -0.36**)
(DVI, RVI)	(0.34**, 0.70**, 0.18*)	(-0.32**, 0.07, -0.06)	(-0.30**, -0.02, -0.02)
(DVI, EVI)	(0.34**, 0.70**, 0.18*)	(-0.60**, -0.01, 0.20**)	(-0.68**, 0.01, 0.24**)
(RVI, EVI)	(-0.23**, 0.23**, 0.30**)	(-0.64**, -0.05, 0.22**)	(-0.65**, -0.04, 0.25**)

Note: The three values from left to right in parentheses show the correlation coefficients at elongation stage, booting stage and flowering stage, respectively

**Table 4:** Model of wheat LNC based on the combinations of two vegetation indexes through different modeling methods

Period	Modeling method	Formula	R <sup>2</sup>
Elongation Stage	Exponential function	$y = 1.4973e^{-0.456x}$	0.60
	Linear function	$y = -0.813x + 1.4879$	0.60
	Logarithmic function	No result.	—
	Polynomial function	$y = 0.9044x^2 - 0.2476x + 1.5236$	0.65
Booting Stage	power function	No result.	—
	Exponential function	$y = 1.4054e^{-2E-04x}$	0.52
	Linear function	$y = -0.0003x + 1.313$	0.52
	Logarithmic function	No result.	—
Flowering stage	Polynomial function	$y = 6E-08x^2 - 7E-05x + 1.5527$	0.52
	power function	No result.	—
	Exponential function	$y = 5.4621e^{-2.245x}$	0.42
	Linear function	$y = -4.1603x + 3.9133$	0.45
	Logarithmic function	$y = -1.6711\ln(x) + 0.6614$	0.41
Flowering stage	Polynomial function	$y = -10.114x^2 + 4.8588x + 1.9753$	0.43
	power function	$y = 0.9505x-0.893$	0.37

Wheat LNC in middle Jiangsu Province was mainly 2.5%–4.5% at elongation stage, 2%–3% at booting stage and about 2.5% at flowering stage, showing a declining trend from the elongation -booting -flowering stages (Fig. 3). These results indicated dynamic nutrient (e.g., nitrogen) circulation in the wheat growth process. Nitrogen flowed to wheat grains as they became increasingly mature. Moreover, maturity of wheat grains could be predicted by changes or difference of LNC at different stages, thus enabling to provide a support to determination of wheat harvest.

## Discussion

Some researchers preferred to evaluate crop growth condition by multiple parameters or combination indicators (Kawamura *et al.*, 2005; Tuia *et al.*, 2011). However, few researches on multi-parameter remote sensing evaluations discussed the correlations among different parameters and internal biological relationships. Most of them concentrated in one fold period, which could not reflect dynamic changes of parameters. Based on these problems, this study analyzed dynamic evaluations of wheat LNC with HJ-CCD images,

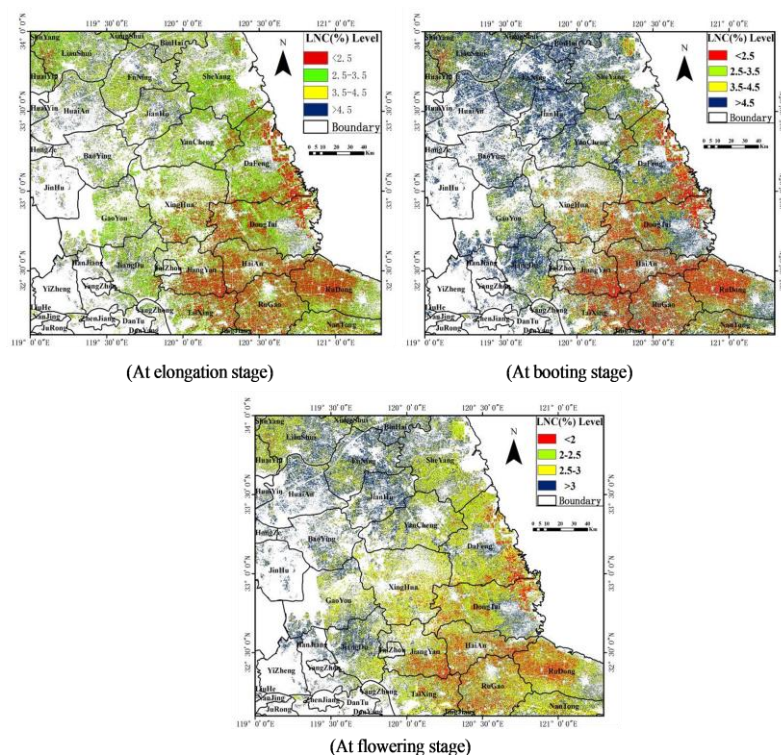


**Fig. 3:** Spatial distribution of wheat LNC in the central region of Jiangsu Province in different periods (Upper: Elongation stage; Middle: Booting stage; Below: Flowering stage)

which disclosed the general dynamic circulation of LNC in wheat growth process and was conducive to studying quality indexes (e.g., nitrogen concentration) of wheat grains in the mature period. Sensitive remote sensing variables of evaluating wheat LNC in different periods were found in the study (Fig. 1), which was one of highlights of this study. Remote sensing evaluations were relatively ideal after the elongation stage of wheat (Bannari *et al.*, 2006; Miyaoka *et al.*, 2012; Kowalik *et al.*, 2014; Tan *et al.*, 2015). Remote sensing evaluations of crop growth mainly focused on existing the relationships between remotely sensed parameters and agronomic indexes (Kawamura *et al.*, 2005; Zhao *et al.*, 2005; Tilling *et al.*, 2007; Daniela *et al.*, 2009; Clevers and Kooistra, 2011; Schlemmer *et al.*, 2013). The involved evaluation models were easy to over rely on a specific remote sensing parameter, but could not cover more remote sensing trait. As a result, although existing models had high accuracy, space-time expansion would need to be improved. When the model accuracy was improved, remote sensing mechanism and repetition were enhanced. The reliability of models was evaluated by measured data. We developed a method for assessing wheat LNC with the combined models on large areas (Fig. 2), which was the second highlight of this study.

Here, wheat LNC data in different crop period were superposed with geographic information. However, surface feature recognition and accurate simultaneous

sampling are susceptible to extreme weather, which will affect LNC evaluation at the field scale (Duncanson *et al.*, 2010). Further studies will focus on physiological reasons of wheat spectral changes with growth stages, and research on eliminating interference, optimize extraction methods, and achieve accurate extraction of wheat-planting area (Duncanson *et al.*, 2010; Erdle *et al.*, 2011). On the other hand, soil, field factors and crop species information should be considered so as to make remote sensing evaluation models more reliable and applicable.

## Conclusion

Applying the models by combining two vegetation indexes could increase the accuracy of assessing LNC at key stages. The LNC at elongation, booting and flowering stages was well correlated with N (SIPI, EVI), D (PSRI, DVI) and N (SIPI, PSRI), respectively, which showed that N (SIPI, EVI), D (PSRI, DVI) and N (SIPI, PSRI) could be successfully employed as potential indicators of accurately assessing LNC at key stages. The combined models were superior to the one fold vegetation index model. The model accuracy increased by 9.9%, 15.2% and 14.7%, respectively. It might also explain the introduction of the compositions of two vegetation indexes into the model of assessing LNC in wheat. All in all, the combined models can not only improve the accuracy of assessing LNC in wheat in key periods, but

also provide a new application method for accurately assessing crops growth status in future.

## Acknowledgements

This work was supported by the National Key Research and Development Program of China (2016YFD0300405), Jiangsu Agricultural Industry Technology System (SXGC[2017]295), the National Natural Science Foundation of China (41271415), a project funded by the Priority Academic Program Development of Jiangsu Higher Education Institutions (PAPD).

## References

- Bagheri, N., H. Ahmadi, S.K. Alavipanah and M. Omid, 2013. Multispectral remote sensing for site-specific nitrogen fertilizer management. *Pesqui. Agropec. Bras.*, 48: 1394–1401
- Bannari, A., A. Pacheco, K. Staenz, H. McNairn and K. Omari, 2006. Estimating and mapping crop residues cover on agricultural lands using hyperspectral and IKONOS data. *Rem. Sens. Environ.*, 104: 447–459
- Boegh, E., R. Houborg, J. Bienkowski and C.F. Braban, 2013. Remote sensing of LAI, chlorophyll and leaf nitrogen pools of crop- and grasslands in five European landscapes. *Biogeoscince*, 10: 6279–6307
- Chen, P., D. Haboudane, N. Tremblay, J. Wang, P. Vigneault and B. Li, 2010. New spectral indicator assessing the efficiency of crop nitrogen treatment in corn and wheat. *Rem. Sens. Environ.*, 114: 1987–1997
- Clevers, J.G.P.W. and L. Kooistra, 2011. *Using Hyperspectral Remote Sensing Data for Retrieving Total Canopy Chlorophyll and Nitrogen Content*, pp: 574–583. The Workshop on Hyperspectral Image & Signal Processing: Evolution in Remote Sensing
- Daniela, S., B. Mirco, B. Pietrolessandro and B. Stefano, 2009. Plant nitrogen concentration in paddy rice from field canopy hyperspectral radiometry. *Field Crop. Res.*, 111: 119–129
- Daughtry, C.S.T., C.L. Walthall, M.S. Kim, E.B.D. Colstoun and M.M. Iii, 2000. Estimating Corn Leaf Chlorophyll Concentration from Leaf and Canopy Reflectance. *Rem. Sens. Environ.*, 74: 229–239
- Duncanson, L.I., K.O. Niemann and M.A. Wulder, 2010. Integration of GLAS and Landsat TM data for aboveground biomass estimation. *Can. J. Rem. Sens.*, 36: 129–141
- Erdle, K., B. Mistele and U. Schmidhalter, 2011. Comparison of active and passive spectral sensors in discriminating biomass parameters and nitrogen status in wheat cultivars. *Field Crop. Res.*, 124: 74–84
- Hatfield, J.L., A.A. Gitelson, J.S. Schepers and C.L. Walthall, 2008. Application of Spectral Remote Sensing for Agronomic Decisions. *Agron. J.*, 100: 117–131
- Inoue, Y., E. Sakaiya, Y. Zhu and W. Takahashi, 2012. Diagnostic mapping of canopy nitrogen content in rice based on hyperspectral measurements. *Rem. Sens. Environ.*, 126: 210–221
- Jacobi, J., W. Kühbauch and J.V. Stafford, 2006. Site-specific identification of fungal infection and nitrogen deficiency in wheat crop using remote sensing. *IEEE International Conference on Geoscience and Remote Sensing Symposium*, pp: 664–667
- Kawamura, K., T. Akiyama, H.O. Yokota, M. Tsutsumi, T. Yasuda, O. Watanabe and S. Wang, 2005. Comparing MODIS vegetation indices with AVHRR NDVI for monitoring the forage quantity and quality in Inner Mongolia grassland, China. *Grassl. Sci.*, 51: 33–40
- Kowalik, W., K. Dabrowska-Zielinska, M. Meroni, T.U. Raczka and A.D. Wit, 2014. Yield estimation using SPOT-VEGETATION products: A case study of wheat in European countries. *Int. J. Appl. Earth Observ. Geoinform.*, 32: 228–239
- Martin, M.E., L.C. Plourde, S.V. Ollinger, M.L. Smith and B.E. Mcneil, 2008. A generalizable method for remote sensing of canopy nitrogen across a wide range of forest ecosystems. *Rem. Sens. Environ.*, 112: 3511–3519
- Miphokasap, P., K. Honda, C. Vaiphasa, M. Souris and M. Nagai, 2012. Estimating canopy nitrogen concentration in sugarcane using field imaging spectroscopy. *Rem. Sens.*, 4: 1651–1670
- Miyaoka, K., M. Maki, J. Susaki, K. Homma, K. Yoshida and C. Hongo, 2012. Detection of rice-planted area using multi-temporal ALOS/PALSAR data. *Geosci. Rem. Sens. Symposium*, pp: 6777–6780
- Morón, A., A. García, J. Sawchik and D. Cozzolino, 2007. Preliminary study on the use of near - infrared reflectance spectroscopy to assess nitrogen content of undried wheat plants. *J. Sci. Food Agric.*, 87: 147–152
- Muharam, F.M., S.A. Maas, K. Bronson and T. Delahunty, 2015a. Estimating cotton nitrogen nutrition status using leaf greenness and ground cover information. *Rem. Sens.*, 7: 7007–7028
- Muharam, F.M., S.J. Maas, K.F. Bronson and T. Delahunty, 2015b. Estimating cotton nitrogen nutrition status using leaf greenness and ground cover information. *Rem. Sens.*, 7: 7007–7028
- Ollinger, S.V., 2011. Sources of variability in canopy reflectance and the convergent properties of plants. *New Phytol.*, 189: 375–394
- Pinter Jr, P.J., J.L. Hatfield, J.S. Schepers, E.M. Barnes, M.S. Moran, C.S.T. Daughtry and D.R. Upchurch, 2003. Remote sensing for crop management. *Photogramm. Eng. Rem. Sens.*, 69: 647–664
- Ree, J., 2006. Run-time calibration of simulation models by integrating remote sensing estimates of leaf area index and canopy nitrogen. *Eur. J. Agron.*, 24: 316–324
- Ryu, C., M. Suguri and M. Umeda, 2011. Multivariate analysis of nitrogen content for rice at the heading stage using reflectance of airborne hyperspectral remote sensing. *Field Crop. Res.*, 122: 214–224
- Schlemmer, M., A. Gitelson, J. Schepers, R. Ferguson, Y. Peng, J. Shanahan and D. Rundquist, 2013. Remote estimation of nitrogen and chlorophyll contents in maize at leaf and canopy levels. *Int. J. Appl. Earth Obsrv. Geoinform.*, 25: 47–54
- Serrano, L., J. Peñuelas and S.L. Ustin, 2002. Remote sensing of nitrogen and lignin in Mediterranean vegetation from AVIRIS data : Decomposing biochemical from structural signals. *Rem. Sens. Environ.*, 81: 355–364
- Tan, C., X. Yang, M. Luo, C. Ma, X. Yan, J. Zhou, Y. Du and Y. Wang, 2015. Using HJ-1A/1B Remote Sensing Images to Monitor Major Growth Indices at Turning Green Stage in Winter Wheat. *J. Trit. Crop.*, 35: 1298–1305
- Tan, C., J. Wang, C. Zhao, Y. Wang, J. Wang, L. Tong, X. Zhu and W. Guo, 2011. Monitoring wheat main growth parameters at anthesis stage by Landsat TM. *Trans. Chin. Soc. Agric. Eng.*, 27: 224–230
- Tarpley, L., K.R. Reddy and G.F. Sassenrathcole, 2000. Reflectance indices with precision and accuracy in predicting cotton leaf nitrogen concentration. *Crop Sci.*, 40: 1814–1819
- Tilling, A.K., G.J. O'Leary, J.G. Ferwerda, S.D. Jones, G.J. Fitzgerald, D. Rodriguez and R. Belford, 2007. Remote sensing of nitrogen and water stress in wheat. *Field Crop. Res.*, 104: 77–85
- Tuia, D., J. Verrelst, L. Alonso, F. Perez-Cruz and G. Camps-Valls, 2011. Multioutput Support Vector Regression for Remote Sensing Biophysical Parameter Estimation. *IEEE Geosci. Rem. Sens. Lett.*, 8: 804–808
- Xu, X., J. Wang, W. Huang, C. Li, X. Yang and X. Gu, 2009. Estimation of crop yield based on weight optimization combination and multi-temporal remote sensing data. *Trans. Chin. Soc. Agric. Eng.*, 25: 137–142
- Zhao, D., K.R. Reddy, V.G. Kakani and V.R. Reddy, 2005. Nitrogen deficiency effects on plant growth, leaf photosynthesis, and hyperspectral reflectance properties of sorghum. *Eur. J. Agron.*, 22: 391–403

(Received 30 March 2018; Accepted 07 May 2018)